

Beat on Gaze: Learning Stylized Generation of Gaze and Head Dynamics

Chengwei Shi
Beihang University
Beijing, China
shichengwei@buaa.edu.cn

Xin Tong
Beihang University
Beijing, China
22371101@buaa.edu.cn

Chong Cao
Beihang University
Beijing, China
chong@buaa.edu.cn

Xukun Shen
Beihang University
Beijing, China
xkshen@buaa.edu.cn

Abstract

Head and gaze dynamics are crucial in expressive 3D facial animation for conveying emotion and intention. However, existing methods frequently address facial components in isolation, overlooking the intricate coordination between gaze, head motion, and speech. The scarcity of high-quality gaze-annotated datasets hinders the development of data-driven models capable of capturing realistic, personalized gaze control. To address these challenges, we propose StyGazeTalk, an audio-driven method that generates synchronized gaze and head motion styles. We extract speaker-specific motion traits from gaze-head sequences with a multi-layer LSTM structure incorporating a style encoder, enabling the generation of diverse animation styles. We also introduce a high-precision multimodal dataset comprising eye-tracked gaze, audio, head pose, and 3D facial parameters, providing a valuable resource for training and evaluating head and gaze control models. Experimental results demonstrate that our method generates realistic, temporally coherent, and style-aware head-gaze motions, significantly advancing the state-of-the-art in audio-driven facial animation. Upon acceptance, we will release our dataset and code to support future research.

1 Introduction

Realistic and expressive 3D facial animation is increasingly vital for a wide range of applications, such as film making, social virtual reality and games. Although recent methods have made progress in modeling lip sync and lower-face expression, they often fall short of capturing the full spectrum of communicative cues required for natural interaction. Among these, gaze and head motions remains particularly ignored, despite its fundamental role in the transmission of intention, emotion, and social presence [25].

Early approaches to gaze generation often relied on hand-crafted rules or fixed procedures, synthesizing gaze behavior based on dialogue structure, speaker roles, and visual saliency cues [19, 20, 29, 35]. While these systems provided valuable semantic interpretability, they struggled to model the rich temporal dynamics and individual variability inherent in natural gaze behavior. In contrast, recent data-driven methods have significantly expanded the scope of facial animation, but they still process facial components in isolation, neglecting the crucial temporal and structural coordination between gaze, head motion, and speech [9, 13, 43, 44, 47]. Moreover, numerous approaches rely on vision-based estimations of facial

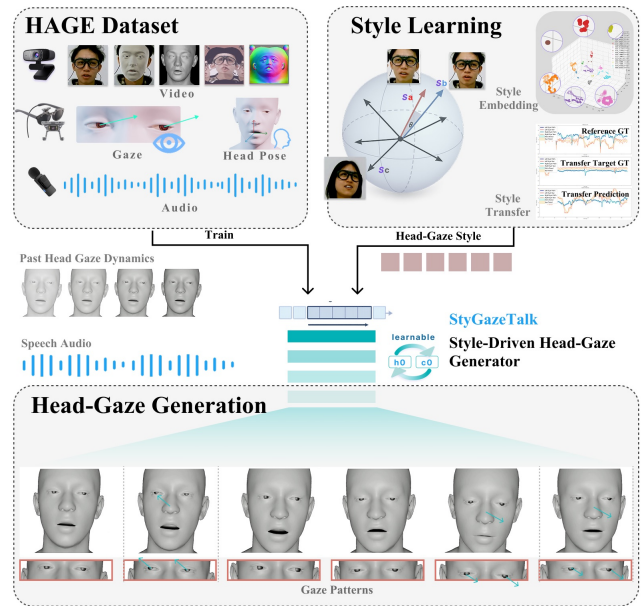


Figure 1: We generate 3D gaze-head motion from audio using a pattern-aware, style-controllable model trained on our high-precision HAGE dataset.

parameters from monocular video [14, 40, 43] and speaker style is often encoded using discrete identity labels [13, 31, 44]. Consequently, these constraints limited the generation of realistic, temporally coherent, and stylistically diverse gaze-head motion, highlighting the need for novel approaches that address these fundamental limitations. To address this limitation and complete the missing gaze motor modality, we build a high-quality multi-modal dataset that includes precisely tracked head and gaze motion from real speakers, collected using a high-precision eye tracker, microphone and camera. Unlike existing datasets that estimate facial parameters from 2D video, our dataset provides direct, high-resolution gaze and head pose measurements.

Realistic gaze generation requires capturing its structured temporal dynamics. Human gaze follows patterns like fixations and saccades, and is tightly coordinated with head motion for stable visual communication [16, 18, 27, 37, 39]. To model this, we use

high-fidelity gaze data and a temporal sequence framework that aligns speech with synchronized gaze-head motion—treating gaze not as isolated parameters but as a coherent modality coupled with audio and head movement.

To enable style-controllable generation, we introduce a contrastive style encoder that learns continuous and interpretable motion representations. Unlike prior works [8, 9, 13, 17, 24, 31, 36, 41, 44, 45] using one-hot speaker embeddings, our method supports fine-grained control and generalization through a latent style space.

To assess gaze behavior beyond regression accuracy, we introduce pattern-level metrics—fixation ratio and gaze-head compensation—inspired by findings in eye movement research. These metrics better reflect perceptual realism and help evaluate whether the model produces gaze dynamics that resemble human behavior.

As shown in 1, our contributions are summarized as follows:

- We present StyGazeTalk, a temporal generation framework that synchronizes 3D gaze and head motion from speech. It captures temporal dependencies across modalities, enabling the model to produce realistic motion that conforms to natural gaze patterns and head dynamics.
- We construct HAGE, the first high-precision dataset to capture synchronized gaze, head pose, audio, and expression in natural face-to-face conversations using professional eye tracking. We further propose pattern-aware evaluation metrics grounded in eye movement research.
- We propose a style encoder that models gaze-head motion styles for personalized generation and enables cross-character style transfer of motion dynamics.

2 Related Work

Recent talking-head methods achieve impressive facial animation, but still face key limitations. We review related work in three areas: speech-driven 3D animation, head pose generation, and style modeling for personalized motion.

2.1 Speech-Driven 3D Facial Animation

Parametric face models provide a compact and controllable representation for 3D facial animation, making them a popular choice for modern data-driven synthesis. Early systems [1, 5, 21, 30] introduced structured representations based on expression or anatomical priors. Among these, the FLAME model [23] has become widely adopted due to its disentangled low-dimensional parameters for identity, expression, and head pose. It supports both reconstruction and animation, offering a flexible foundation for learning-based generative frameworks. In our work, we leverage FLAME to represent our facial animation.

Recent advances have extended these models to build speech-driven facial animation pipelines. Approaches like CodeTalker [44], VOCA [9], and MeshTalk [32] predict facial expressions and lip motion from audio input, often using pretrained encoders such as Wav2Vec2 [2] to extract temporally rich features. These methods have achieved impressive results in lip synchronization and speech alignment. However, most of them focus on the lower face and fail to model full-face dynamics, particularly head motion and eye gaze—two critical modalities that convey attention, emotion, and

communicative intent. Moreover, facial components are often modeled in isolation, lacking the temporal and structural coordination necessary for naturalistic and expressive talking-head animation.

2.2 Head Pose Generation

Head motion generation from speech is central to audio-driven facial animation, with both 2D and 3D approaches enhancing realism and expressiveness. 2D methods like MakeItTalk [47], Audio2Head [43], and SadTalker [45] synthesize head motion via key-point warping or dense flow in image space, but often lack explicit 3D control and are sensitive to pose and occlusion. In contrast, 3D approaches such as DiffPoseTalk [40] and FaceFormer [13] regress structured head pose parameters (e.g., Euler angles) from audio, supporting better view generalization and applications in AR/VR. However, both paradigms suffer from weak supervision: popular datasets like VoxCeleb [28] and HDTF [45] lack sensor-based ground truth, relying instead on vision-based pose estimators [3, 14, 15, 26]. These estimators fit 3DMMs to landmarks or dense proxies, but are prone to noise, temporal drift, and expression entanglement—especially under occlusion, extreme poses, or low resolution—leading to jittery or over-smoothed results and limited generalization across speakers or emotions.

2.3 Style Modeling

Many existing talking-head systems use one-hot speaker IDs to represent motion style [8, 9, 13, 17, 24, 31, 36, 41, 45]. However, this approach treats style as a discrete attribute, ignoring inter-speaker similarity and intra-speaker variability. To overcome these limitations, recent work has explored learning continuous style embeddings from data. For example, Chen et al. [6] use contrastive loss to align positive pairs while separating negatives; CL-MEx [34] applies a similar idea to learn view-invariant facial features; Vi2CLR [11] jointly learns image and video embeddings via clustering and similarity. Inspired by these methods, we adopt a contrastive style encoder to capture individualized gaze-head dynamics, replacing discrete IDs with learnable and generalizable representations.

3 Method

An overview of our method is shown in Figure 2. Our goal is to generate temporally coherent and stylistically expressive 3D gaze-head motion from speech. Gaze behavior is structured and time-varying, with both short-term fluctuations and long-term trends (Section 3.2), and is tightly coupled with head motion and audio. To model this complexity, we treat it as a speech-conditioned temporal generation task, using a sliding-window, multi-layer LSTM with a style encoder. This design captures local dynamics and preserves global stylistic consistency, enabling natural motion aligned with speech.

3.1 Problem Formulation

Let $\mathbf{A}_{1:T} = (\mathbf{a}_1, \dots, \mathbf{a}_T)$ denote a sequence of audio features extracted from raw speech, where each $\mathbf{a}_t \in \mathbb{R}^d$ is a d -dimensional embedding. Let $\mathbf{X}_{1:T} = (\mathbf{x}_1, \dots, \mathbf{x}_T)$ be the corresponding motion sequence, where each $\mathbf{x}_t \in \mathbb{R}^7$ includes 3D head rotation (pitch, yaw, roll) and binocular gaze angles (left/right pitch and yaw). Our

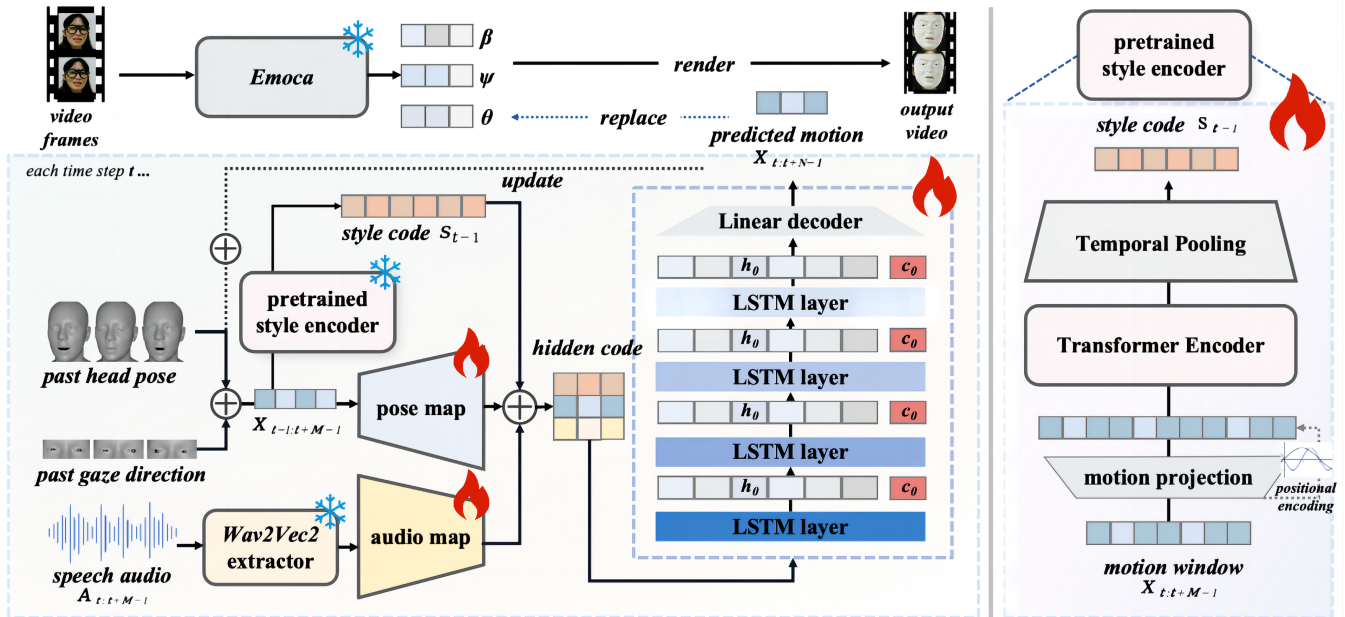


Figure 2: Overview of our method. (Left) At each time step t , the model takes audio $A_{t:t+M}$, past motion $X_{t-1:t+M}$, and a style code S_{t-1} , and predicts future motion $X_{t:t+N-1}$ using a conditional sequence generation model. (Right) The style code is extracted from past motion via a pretrained Transformer encoder, enabling style-aware, temporally coherent motion generation.

goal is to learn a function that sequentially maps audio to motion, conditioned on a specific motion style.

At each time step t , the model takes as input an audio segment $A_{t:t+M-1}$ and a motion segment $X_{t-1:t+M-1}$ of length M , along with a style embedding s_{t-1} extracted from the preceding motion window. It then predicts the future motion segment $X_{t:t+N-1}$ of length N .

3.2 Pattern-Informed Generation

Unlike arbitrary or noise-like signals, gaze behavior exhibits structured and interpretable dynamics. Drawing on insights from eye movement research [4, 16, 18, 27, 37–39], we decompose gaze-head motion into two complementary components, as illustrated in Figure 3.

(1) **Shared patterns** capture universal temporal characteristics across speakers. These include long-term trends such as head-gaze coupling, where the eyes and head move in a coordinated manner to maintain visual attention, and short-term fluctuations like fixations (velocity $< 30^\circ/s$) and saccades (velocity $> 30^\circ/s$) [4, 38].

(2) **Sample-specific patterns** capture motion styles that exhibit consistency within a short temporal window of the same individual. Adjacent segments from the same subject and session often exhibit coherent stylistic traits, such as dynamic velocity and motion amplitude patterns.

To effectively capture both shared and sample-specific motion patterns, our generation framework integrates two key components. For shared patterns, we use a multi-layer LSTM with learnable initial hidden and cell states, enabling each generation window to start from an optimized prior memory and better model long-term motion trends and head-gaze coordination. For sample-specific traits,

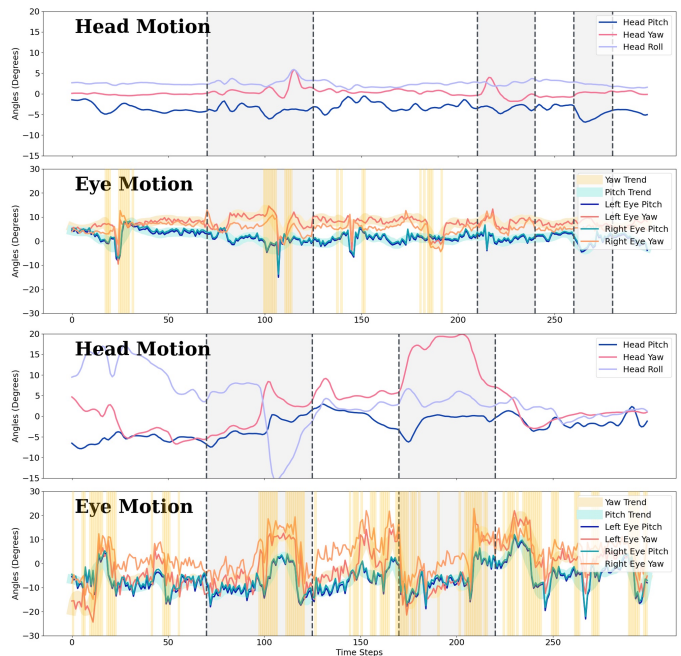


Figure 3: Illustration of structured gaze-head motion dynamics across speakers and sessions. The examples highlight short-term fluctuations—such as saccades (yellow) and fixations—long-term coordination patterns (gray regions), and stylistic differences in gaze-head dynamics across individuals.

we adopt a sliding-window generation strategy with a style encoder, which extracts personalized dynamics from preceding segments to condition each window. This enables stable and flexible generation, especially for variable-length speech and real-time applications. To learn coordinated inter-modal dynamics, we concatenate head and eye motion features into a unified sequence. We choose LSTM over Transformer architectures due to both data scale and application constraints. While Transformers are powerful for global dependency modeling, their high complexity and reliance on large-scale data and full-sequence input can lead to overfitting in our context [12]. In contrast, our multi-layer LSTM design effectively captures both high-level temporal patterns and fine-grained dynamics. Ablation studies (Section 5 and supplementary materials) validate its advantage over Transformer-based alternatives.

3.3 Synthesis of Gaze-Pose Dynamics

Specifically, we adopt the architecture of the state-of-the-art self-supervised speech model Wav2Vec 2.0 [2], which consists of a temporal convolutional feature extractor followed by a multi-layer Transformer encoder. For each time step t , we extract a window of contextualized audio features $\mathbf{A}_{t:t+M-1}$ from the raw waveform input $\mathbf{A}_{1:T} = (\mathbf{a}_1, \dots, \mathbf{a}_T)$. These features are then projected into a d -dimensional space via a learnable linear layer, yielding $\tilde{\mathbf{A}}_{t:t+M-1} \in \mathbb{R}^{M \times d}$.

Simultaneously, the previous motion window $\mathbf{X}_{t-1:t+M-1} \in \mathbb{R}^{M \times 7}$ is encoded into the same latent space, resulting in $\tilde{\mathbf{X}}_{t-1:t+M-1} \in \mathbb{R}^{M \times d}$. To incorporate individualized motion styles, we apply a pretrained style encoder (introduced in Section 3.4) to the same segment, extracting a style vector $\mathbf{s}_{t-1} \in \mathbb{R}^{d_s}$:

$$\mathbf{s}_{t-1} = \text{SE}(\mathbf{X}_{t-1:t+M-1}).$$

To integrate multi-modal information in a unified representation, the encoded audio features, motion features, and style vector are concatenated along the feature dimension to form the generator input: $\mathbf{Z}_t \in \mathbb{R}^{M \times (2d+d_s)}$. This concatenation enables the model to jointly consider speech content, motion history, and personalized style within each generation window, facilitating coherent and style-aware motion prediction.

To effectively model both global trends and fine-grained dynamics, we employ a multi-layer LSTM architecture, where each layer captures motion patterns at a different temporal scale. Crucially, the LSTM is initialized with learnable hidden and cell states $(\mathbf{h}_0, \mathbf{c}_0)$, allowing the model to adaptively encode modality-aware priors and maintain temporal coherence across prediction windows. This design processes the fused sequence \mathbf{Z}_t to predict the future motion segment as:

$$\hat{\mathbf{X}}_{t:t+N-1} = \text{MG}(\mathbf{Z}_t; \mathbf{h}_0, \mathbf{c}_0),$$

where N is the prediction length and $\text{MG}(\cdot)$ denotes our Motion Generator.

While our model focuses solely on generating dynamic gaze and head motion, we optionally combine the output with shape, jaw pose, and expression parameters extracted using EMOCA [10] during the inference stage. This fusion is used for visualization purposes to produce complete and animatable face representations, and does not influence model training or prediction.

We use a combination of position and motion losses to train the model.

MSE Loss. To ensure frame-wise accuracy, we apply a mean squared error loss:

$$\mathcal{L}_{\text{mse}} = \frac{1}{T} \sum_{t=1}^T \|\hat{\mathbf{x}}_t - \mathbf{x}_t\|_2^2 \quad (1)$$

Velocity Loss. To better capture motion dynamics, we introduce a velocity loss:

$$\mathcal{L}_{\text{vel}} = \frac{1}{T-1} \sum_{t=2}^T \|(\hat{\mathbf{x}}_t - \hat{\mathbf{x}}_{t-1}) - (\mathbf{x}_t - \mathbf{x}_{t-1})\|_2^2 \quad (2)$$

This helps model realistic transitions like saccades and gaze-head coordination.

The final objective combines both terms:

$$\mathcal{L}_{\text{gen}} = \lambda \cdot \mathcal{L}_{\text{mse}} + (1 - \lambda) \cdot \mathcal{L}_{\text{vel}} \quad (3)$$

where λ_{mse} and λ_{vel} control the trade-off between position and motion.

3.4 Style Encoder

To model subject-specific motion styles, we introduce a style encoder that extracts a fixed-length style vector from a short motion segment, based on the observation that adjacent segments from the same speaker share stylistic traits.

Given an input window $\mathbf{X} \in \mathbb{R}^{M \times 7}$, we first apply a linear projection and temporal encoding:

$$\mathbf{X}' = \text{MTE}(\text{Linear}(\mathbf{X})) \in \mathbb{R}^{M \times d}.$$

The sequence is then processed by a Transformer encoder \mathcal{T}_θ , followed by average pooling to obtain a global style embedding:

$$\mathbf{s} = \frac{1}{M} \sum_{i=1}^M \mathcal{T}_\theta(\mathbf{X}')_i \in \mathbb{R}^{d_s}.$$

We train the encoder using the NT-Xent contrastive loss [6]. Positive pairs are formed from adjacent segments of the same speaker, and negatives come from different speakers or distant times. For a batch of N samples, we collect all style embeddings as $\mathcal{S} = \{\mathbf{s}_1^a, \dots, \mathbf{s}_N^a, \mathbf{s}_1^b, \dots, \mathbf{s}_N^b\} \in \mathbb{R}^{2N \times d_s}$, and define cosine similarity as $\text{sim}(\mathbf{s}_i, \mathbf{s}_j) = \frac{\mathbf{s}_i^T \mathbf{s}_j}{\|\mathbf{s}_i\| \cdot \|\mathbf{s}_j\|}$.

The contrastive loss is:

$$\mathcal{L}_{\text{con}} = - \sum_{i=1}^{2N} \log \frac{\exp(\text{sim}(\mathbf{s}_i, \mathbf{s}_{p(i)})/\tau)}{\sum_{k=1, k \neq i}^{2N} \exp(\text{sim}(\mathbf{s}_i, \mathbf{s}_k)/\tau)}$$

where τ is a temperature hyperparameter.

This objective promotes temporal consistency within the same speaker and separation across different styles, resulting in stable and generalizable style control during motion generation.

4 HAGE Dataset

The Head Pose–Audio–Gaze–Expression (HAGE) dataset is a high-precision multimodal corpus for modeling natural gaze-motor dynamics in conversation. It contains ~2.5 hours of curated recordings from 8 subjects (male and female), contributing unscripted Chinese and English dialogue. The dataset provides tightly synchronized

16kHz audio, binocular gaze, 3D head rotations, and 1080×1080 video. All motion data—including head pose, gaze angles, and 3D facial parameters are aligned to 25 FPS. As the first face-to-face talking dataset with professional eye-tracker-captured gaze, HAGE supports temporally coherent and context-aware modeling of head-gaze coordination during natural speech.

Dataset	Audio	Video	Head Pose	Gaze	Expression	Data Acquisition	Content
VOCASET	✓	✓	✓	✗	✓	4D Scans	Scripted
MEAD	✓	✓	✗	✗	✓	RGB	Scripted
BIWI	✓	✓	✓	✗	✗	RGB-D	None
TFHP	✓	✓	✓	✗	✓	RGB	Formal Video
HAGE(ours)	✓	✓	✓	✓	✓	Eye Tracker	Unscripted

Table 1: Multimodal Dataset Comparison.

Comparison of Datasets. Table 1 summarizes existing talking-face datasets. Most lack gaze data or rely on scripted speech or vision-based estimation. In contrast, our HAGE dataset uniquely provides synchronized audio, video, 3D head pose, gaze, and expression from unscripted conversations, captured with high-precision sensors—supporting natural and expressive head–gaze dynamics.[42]

4.1 Settings and Postprocessing

We collected data in a controlled indoor setup where each subject wore a Pupil Labs eye tracker and engaged in unscripted conversations. The system recorded 100Hz 3D gaze, 33Hz head pose (quaternions), 1080×1080 video, and 41kHz audio, synchronized via a custom program using the Pupil Labs API and OpenCV. We manually extracted valid segments, aligned gaze/head data to 25 FPS, converted them to angular form, and enhanced the audio. Frames with extreme angles ($\pm 40^\circ$) were removed for stable learning. See our supplementary for details.

4.2 Gaze Pattern Metrics

To evaluate the realism of gaze-head dynamics, we adopt three metrics: Fixation Ratio, Compensation Score, and Similarity with Ground Truth (SimWithGT). These capture both structural and dynamic aspects of gaze motion.

4.2.1 Fixation Ratio. We use a dispersion-based I-DT algorithm [37] to detect fixations from binocular gaze angles (left/right eye pitch and yaw). Angular dispersion D within a sliding window is defined as:

$$D = \max(x) - \min(x) + \max(y) - \min(y), \quad (4)$$

where x and y are yaw and pitch across both eyes. A window is considered a fixation if $D \leq 3.5$ and lasts at least 3 consecutive frames [33]. Each frame is thus labeled as either fixation or saccade, and the fixation ratio is:

$$\text{FixRatio} = \frac{N_{\text{fixation}}}{N_{\text{fixation}} + N_{\text{saccade}}}, \quad (5)$$

where N_{fixation} and N_{saccade} denote the number of frames identified as fixation and saccade, respectively.

4.2.2 Compensation Score. Following [16], we assess eye-head coordination by comparing head velocity $\bar{\mathbf{h}}_t$ and average eye velocity

$\bar{\mathbf{e}}_t$. Net gaze shift is $\mathbf{g}_t = \bar{\mathbf{e}}_t + \bar{\mathbf{h}}_t$. The score per frame is:

$$\text{Score}_t = \begin{cases} -\|\bar{\mathbf{h}}_t\|, & \|\mathbf{g}_t\| < 20 \\ -\cos(\theta), & 25 \leq \|\mathbf{g}_t\| \leq 90 \\ 0, & \text{otherwise} \end{cases} \quad (6)$$

where θ is the angle between $\bar{\mathbf{h}}_t$ and $\bar{\mathbf{e}}_t$. Final score is:

$$\text{CompScore} = \frac{1}{T} \sum_{t=1}^T \text{Score}_t. \quad (7)$$

4.2.3 Similarity with Ground Truth. To assess overall realism, we define the similarity-with-ground-truth score as:

$$\text{Sim} = 1 - (|\text{Fix}_{\text{GT}} - \text{Fix}_{\text{pred}}| + |\text{Comp}_{\text{GT}} - \text{Comp}_{\text{pred}}|). \quad (8)$$

Higher scores indicate closer alignment in both gaze fixation patterns and gaze-head coordination.

5 Experiments

5.1 General Evaluation

To evaluate the effectiveness of our approach, we conduct extensive comparisons on our dataset. We first perform ablation studies to assess the contribution of each component, including the base LSTM model (Base), style encoders of different dimensions (SE-32/SE-64), a Transformer-based generation model (TFM-SE-64) that replaces the original LSTM, with architecture and hyperparameters carefully adjusted to ensure fair comparison, and a version that uses MPI-IGaze [7] instead of our high-precision eye-tracking data for the initial motion window (MPGW). For baseline comparison, as our task focuses on joint gaze and head pose generation, we compare with five publicly available audio-driven head motion methods: SadTalker [45], DiffPoseTalk [40], Audio2Head [43], PC-AVS [46], and MakeltTalk [47]. Since none of them generate gaze, the comparison is limited to head pose metrics. We report five key metrics for head and gaze motion, including three angle-based ones: Mean Absolute Error (MAE), Velocity Error (Vel), and Motion Energy Error (MEE), and Beat Alignment Score (BAS), as introduced in [22], which measures the temporal alignment between motion beats and speech rhythm. These metrics collectively assess positional accuracy, motion dynamics, and synchronization with audio.

As shown in Table 2, our full model with 64 dimension of style encoder (SE-64) achieves the lowest MAE, as well as the lowest overall MEE, highlighting the effectiveness of the style encoder in boosting precision and capturing dynamic, style-consistent motion. The addition of velocity loss (SE-64-VEL) improves velocity (6.715) and BAS (0.243), suggesting velocity loss can enhance dynamic and more natural audio-motion coordination. (TFM-SE-64) results in degraded performance, particularly on gaze metrics, suggesting its limited ability to capture temporal head-gaze dynamics. Under noisy, vision-estimated motion inputs (MPGW), the substantial drop highlights the critical benefit of using high-precision motion data as input for learning fine-grained gaze–head dynamics. Compared to baselines without gaze modeling, our method achieves lower head MAE and better BAS. While *DiffPoseTalk* performs well on head dynamics, it omits gaze. In contrast, our joint modeling of gaze and head motion produces more expressive and coordinated behavior, as shown in qualitative results and user studies.

	Section	All					Gaze				Head			
	Metric	MAE↓	Vel↓	MEE↓	CE↓	BAS↑	MAE↓	Vel↓	MEE↓	BAS↑	MAE↓	Vel↓	MEE↓	BAS↑
Ablation	Base	5.149	6.840	57.350	0.139	0.219	6.616	11.888	57.174	0.205	3.193	0.108	0.398	0.211
	SE-32	5.097	6.863	56.836	0.138	0.221	6.527	11.928	56.655	0.231	3.189	0.109	0.403	0.207
	SE-64	5.087	6.843	56.411	0.136	0.236	6.535	11.894	56.215	0.238	3.156	0.107	0.390	0.205
	SE-64-VEL	5.219	6.715	56.616	0.152	0.243	6.645	11.668	56.445	0.240	3.317	0.112	0.413	0.212
	TFM-SE-64	5.659	7.852	71.177	0.137	0.197	7.353	13.618	70.938	0.199	3.400	0.166	0.611	0.203
	MPGW	6.013	7.038	56.944	0.876	0.208	7.608	12.231	56.727	0.211	3.887	0.114	0.415	0.206
Head-only	SadTalker	-	-	-	-	-	-	-	-	-	3.935	0.173	0.618	0.199
	DiffPoseTalk	-	-	-	-	-	-	-	-	-	4.415	0.093	0.327	0.199
	Audio2Head	-	-	-	-	-	-	-	-	-	5.810	0.175	0.648	0.193
	PC-AVS	-	-	-	-	-	-	-	-	-	3.937	0.199	0.719	0.197
	MakeItTalk	-	-	-	-	-	-	-	-	-	3.939	0.211	0.766	0.198

Table 2: Quantitative evaluation of the ablation models and baselines.

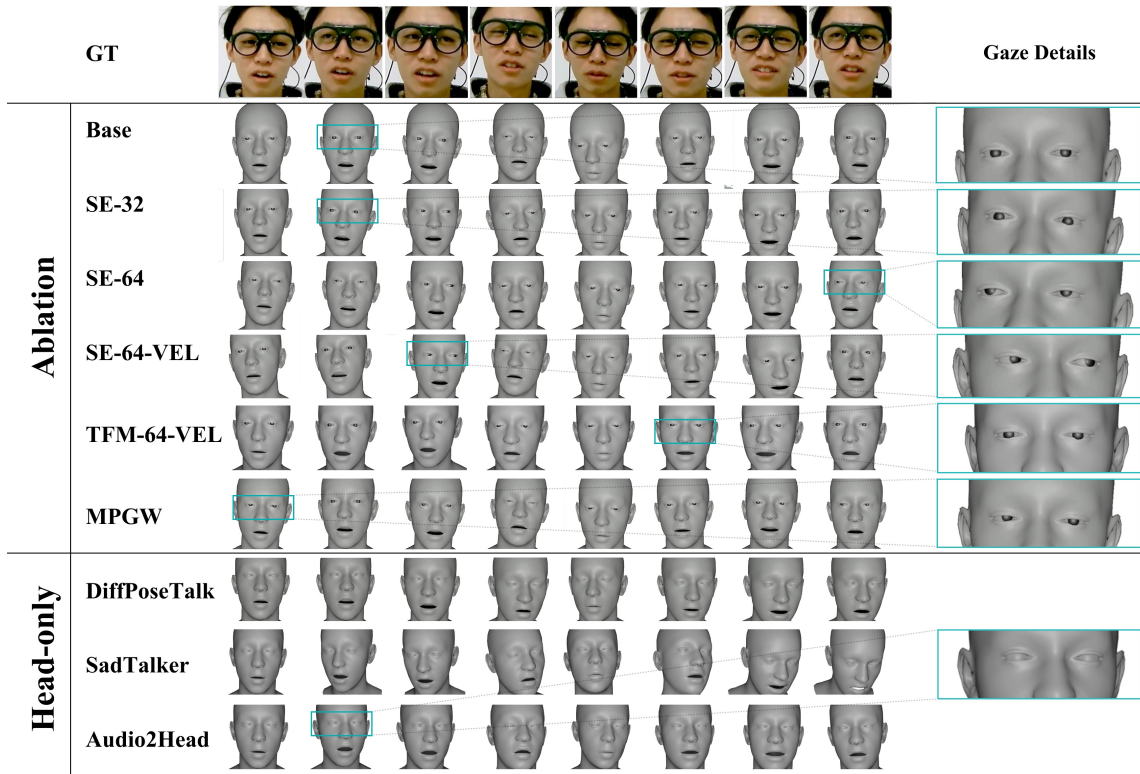


Figure 4: Visual results of ablation study of our methods and qualitative comparison of state-of-the-art methods.

Figure 4 shows qualitative comparisons across baselines and ablations. Our full model produces more vivid, natural gaze-head motion than head-only baselines. For head-only methods like DiffPoseTalk, eye render is omitted to avoid confusion. Even the base model benefits from unified modeling, generating plausible head-eye motion. Adding the style encoder (*SE-32/SE-64*) improves naturalness and

expressiveness, with *SE-64* showing stronger stylistic cues. Velocity loss (*SE-64-VEL*) further enhances motion richness. In contrast, *TFM-SE-64* yields over-smoothed and less meaningful motion, revealing limitations in capturing gaze dynamics. Vision-initialized *MPGW* suffers from unstable gaze. These results confirm the effectiveness

of our style-aware, physiologically grounded framework. More details are demonstrated in our perceptual study and supplementary materials

5.2 Gaze Pattern Evaluation

Section	saccades	fixation	compScore	simScore
GT	38.87%	61.13%	-0.3366	1
Base	25.83%	74.17%	-0.2890	0.8220
SE-32	29.02%	70.98%	-0.3021	0.8670
SE-64	30.78%	69.22%	-0.3054	0.8879
SE-64-vel	32.67%	67.33%	-0.3100	0.9114
TFM-SE-64	15.43%	84.57%	-0.2006	0.6296
MPGW	24.28%	75.72%	-0.3860	0.8047

Table 3: Results of gaze pattern evaluation.

Table 3 summarizes results across fixation ratio, compensation score, and the composite SimScore. Ground-truth motion shows a fixation ratio of 61.13% and a compensation score of -0.3366 , consistent with conversational gaze patterns [33]. The *Base* model over-predicts fixations (74.17%) and underestimates coordination (-0.2890), yielding a SimScore of 0.8220. Adding a style encoder (*SE-32*) improves realism and coordination (SimScore: 0.8670), with *SE-64* further enhancing performance (0.8879). Velocity supervision in *SE-64-VEL* leads to the best alignment (0.9114), balancing fixation and dynamic consistency. In contrast, *TFM-SE-64* over-smooths gaze (84.57%, SimScore: 0.6296), and *MPGW* shows rigid gaze behavior (0.8047), highlighting the value of accurate gaze modeling.

5.3 Style Encoder Evaluation

We evaluate the effectiveness of our style encoder through three experiments: style similarity scoring, clustering visualization, and style transfer.

5.3.1 Style Encoder Metrics. To evaluate how well the style encoder captures individual motion characteristics, we compute the cosine distance between style embeddings of predicted and ground-truth motion windows. Given normalized motion windows, we extract style embeddings using the pretrained encoder and define cosine error as $\mathcal{E}_{\text{style}} = 1 - \cos(\mathbf{s}^{\text{gt}}, \hat{\mathbf{s}})$. This metric reflects how well the predicted motion preserves stylistic traits such as gaze intensity, rhythm, and head movement patterns. A lower value indicates better style alignment. We report the average error across all sliding windows. As shown in Table 2 (CE: cosine error), *Base* gives 0.139. Style supervision (*SE-32*) lowers this to 0.138, and *SE-64* further improves it to 0.136. The vision-based baseline (*MPGW*) gives the highest error (0.876), confirming the benefit of our precise motion data.

5.3.2 Clustering Visualization. Figure 5 shows t-SNE results over 10 test sessions. Ground-truth embeddings form distinct clusters by session, and predicted embeddings are closely aligned—demonstrating that the style encoder captures consistent, session-specific dynamics even from generated motion.

5.3.3 Style Transfer. Figure 6 illustrates effective style transfer, where the generated motion preserves the target’s content while

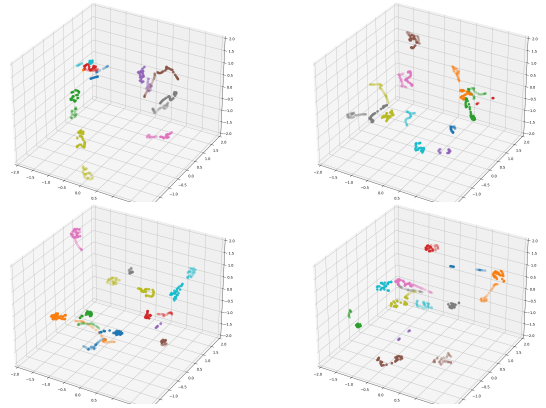


Figure 5: t-SNE visualization of style embeddings. Each color denotes a test session; solid points are ground truth, transparent ones are predictions.

adopting the source’s stylistic dynamics. This demonstrates the capability of our style encoder to disentangle style from content, enabling identity-agnostic and flexible control. Additional results are provided in the supplementary video.

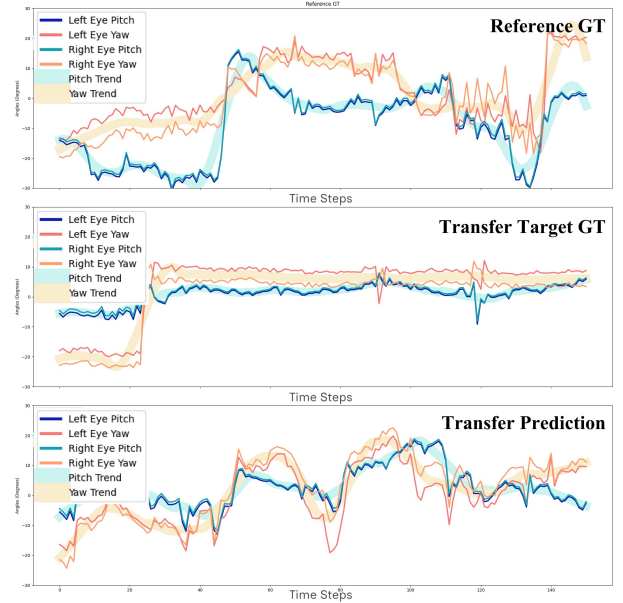


Figure 6: Style Transfer. The prediction captures the temporal style of the reference while preserving the target’s style structure.

5.4 User Perception Study

To assess the perceptual quality of our generated gaze-head motion, we conducted a user study comparing our method (*SE-64*) with two baselines: *DiffPoseTalk* (strongest head-motion baseline) and *TFM-SE-64*. Participants watched 12 short videos (10 test, 2 verification) and answered six single-choice questions per video, covering three aspects—*Naturalness*, *Realism*, and *Style Similarity*—with two questions per aspect. Each question required choosing the most

convincing result among the three methods. We recruited 88 participants and retained 78 valid responses after consistency checks (see supplementary). As shown in Table 4, our method received the highest user preference across all three perceptual dimensions, notably in naturalness and style similarity. While *TFM-SE-64* benefits from style encoding, it suffers from reduced motion realism. *DiffPoseTalk*, which lacks gaze modeling, performed worst overall. These results highlight our method’s superior balance of dynamic realism and personalized motion style in speech-driven gaze–head generation. For more details, please refer to our supplementary materials.

Method	Naturalness	Realism	Style Similarity
DiffPoseTalk	24.5%	26.2%	24.4%
TFM-SE-64	27.2%	25.3%	27.6%
SE-64 (Ours)	48.3%	48.5%	47.9%

Table 4: User preference distribution (%) across three perceptual dimensions.

6 Conclusion

We present *StyGazeTalk*, a speech-driven framework for generating realistic head-gaze motion. It supports real-time, synchronized output and is trained on a high-precision dataset with rich gaze-head annotations. Future work includes hybrid training, semantic integration, and cross-domain adaptation.

Acknowledgements

This work was supported by Beijing Natural Science Foundation (No. QY24127).

References

[1] Itimad Ali, Ghazali Sulong, and Hoshang Kolivand. 2015. Realistic Lip Syncing for Virtual Character Using Common Viseme Set. *Computer and Information Science* 8 (07 2015), 71–71. DOI: <http://dx.doi.org/10.5539/cis.v8n3p71>

[2] Alexei Baevski, Henry Zhou, Abdelrahman Mohamed, and Michael Auli. 2020. wav2vec 2.0: A Framework for Self-Supervised Learning of Speech Representations. (2020). <https://arxiv.org/abs/2006.11477>

[3] Tadas Baltrušaitis, Peter Robinson, and Louis-Philippe Morency. 2016. OpenFace: An open source facial behavior analysis toolkit. In *2016 IEEE Winter Conference on Applications of Computer Vision (WACV)*. 1–10. DOI: <http://dx.doi.org/10.1109/WACV.2016.7477553>

[4] Roberto Becerra García, Rodolfo García B., and Gonzalo Joya. 2021. Differentiation of Saccadic Eye Movement Signals. *Sensors* 21 (07 2021), 5021. DOI: <http://dx.doi.org/10.3390/s21155021>

[5] Chen Cao, Yanlin Weng, Shun Zhou, Yiyang Tong, and Kun Zhou. 2014. FaceWarehouse: A 3D Facial Expression Database for Visual Computing. *IEEE Transactions on Visualization and Computer Graphics* 20, 3 (2014), 413–425. DOI: <http://dx.doi.org/10.1109/TVCG.2013.249>

[6] Ting Chen, Simon Kornblith, Mohammad Norouzi, and Geoffrey Hinton. 2020. A Simple Framework for Contrastive Learning of Visual Representations. (2020). <https://arxiv.org/abs/2002.05709>

[7] Yihua Cheng, Hengfei Wang, Zhongqun Zhang, Yang Yue, Bo Eun Kim, Feng Lu, and Hyung Jin Chang. 2025. 3D Prior is All You Need: Cross-Task Few-shot 2D Gaze Estimation. (2025). <https://arxiv.org/abs/2502.04074>

[8] Junie Chung and Andrew Zisserman. 2019. Voice2Face: Real-Time Face Reconstruction with Audio. In *Proceedings of the IEEE Conference on Computer Vision and Pattern Recognition (CVPR)*. 1102–1111. DOI: <http://dx.doi.org/10.1109/CVPR.2019.00117>

[9] Daniel Cudeiro, Timo Bolkart, Cassidy Laidlaw, Anurag Ranjan, and Michael Black. 2019. Capture, Learning, and Synthesis of 3D Speaking Styles. *Computer Vision and Pattern Recognition (CVPR)* (2019), 10101–10111. <http://voca.is.tue.mpg.de/>

[10] Radek Danecek, Michael J. Black, and Timo Bolkart. 2022. EMOCA: Emotion Driven Monocular Face Capture and Animation. In *Conference on Computer Vision and Pattern Recognition (CVPR)*. 20311–20322.

[11] Ali Diba, Vivek Sharma, Reza Safdari, Dariush Lotfi, Saquib Sarfraz, Rainer Stiefelhagen, and Luc Van Gool. 2021. Vi2CLR: Video and Image for Visual Contrastive Learning of Representation. In *Proceedings of the IEEE/CVF International Conference on Computer Vision (ICCV)*. 1502–1512.

[12] Aysu Ezen-Can. 2020. A Comparison of LSTM and BERT for Small Corpus. (2020). <https://arxiv.org/abs/2009.05451>

[13] Yingruo Fan, Zhaojiang Lin, Jun Saito, Wenping Wang, and Taku Komura. 2022. FaceFormer: Speech-Driven 3D Facial Animation with Transformers. In *Proceedings of the IEEE/CVF Conference on Computer Vision and Pattern Recognition (CVPR)*.

[14] Yao Feng, Haiwen Feng, Michael J. Black, and Timo Bolkart. 2021. Learning an Animatable Detailed 3D Face Model from In-The-Wild Images. *ACM Transactions on Graphics, (Proc. SIGGRAPH)* 40, 8 (2021). <https://doi.org/10.1145/3450626.3459936>

[15] Panagiotis P. Filntisis, George Retsinas, Foivos Paraperas-Papantoniou, Athanasios Katsamanis, Anastasios Roussos, and Petros Maragos. 2022. Visual Speech-Aware Perceptual 3D Facial Expression Reconstruction from Videos. (2022).

[16] Edward Freedman and David Sparks. 1997. Eye-Head Coordination During Head-Unrestrained Gaze Shifts in Rhesus Monkeys. *Journal of neurophysiology* 77 (06 1997), 2328–48. DOI: <http://dx.doi.org/10.1152/jn.1997.77.5.2328>

[17] Siddharth Gururani, Arun Malloya, Ting-Chun Wang, Rafael Valle, and Ming-Yu Liu. 2022. SPACE: Speech-driven Portrait Animation with Controllable Expression. (2022). <https://arxiv.org/abs/2211.09809>

[18] Kenneth Holmqvist, Marcus Nyström, and Fiona Mulvey. 2012. Eye tracker data quality: what it is and how to measure it. In *Proceedings of the Symposium on Eye Tracking Research and Applications (ETRA '12)*. Association for Computing Machinery, New York, NY, USA, 45–52. DOI: <http://dx.doi.org/10.1145/2168556.2168563>

[19] Tomoko Koda, Taku Hirano, and Takuto Ishioh. 2017. Development of Culture-specific Gaze Behaviours of Virtual Agents. In *International Conference on Agents and Artificial Intelligence*. <https://api.semanticscholar.org/CorpusID:26499860>

[20] Sooha Park Lee, Jeremy B. Badler, and Norman I. Badler. 2002. Eyes alive. *Proceedings of the 29th annual conference on Computer graphics and interactive techniques* (2002). <https://api.semanticscholar.org/CorpusID:790087>

[21] Joe Letteri. 2023. Technology and Innovation in Avatar: The Way of Water. In *Proceedings of the 2023 Digital Production Symposium (DigiPro '23)*. Association for Computing Machinery, New York, NY, USA, Article 3, 3 pages. DOI: <http://dx.doi.org/10.1145/3603521.3604300>

[22] Ruilong Li, Shan Yang, David A. Ross, and Angjoo Kanazawa. 2021. AI Choreographer: Music Conditioned 3D Dance Generation with AIST++. (2021). <https://arxiv.org/abs/2101.08779>

[23] Tianye Li, Timo Bolkart, Michael J. Black, Hao Li, and Javier Romero. 2017. Learning a model of facial shape and expression from 4D scans. *ACM Transactions on Graphics, (Proc. SIGGRAPH Asia)* 36, 6 (2017), 194:1–194:17. <https://doi.org/10.1145/3130800.3130813>

[24] Yipin Li, Zhenyu Liu, Jiebo Luo, and Zenglin Hu. 2019. FSGAN: Face Swapping Generative Adversarial Network. In *Proceedings of the IEEE International Conference on Computer Vision (ICCV)*. 819–828. DOI: <http://dx.doi.org/10.1109/ICCV.2019.00097>

[25] Kang Liu and Joern Ostermann. 2011. Evaluation of an image-based talking head with realistic facial expression and head motion. *Journal on Multimodal User Interfaces* 5 (03 2011). DOI: <http://dx.doi.org/10.1007/s12193-011-0070-8>

[26] Camillo Lugaresi, Jiuqiang Tang, Hadon Nash, Chris McClanahan, Esha Uboweja, Michael Hays, Fan Zhang, Chuo-Ling Chang, Ming Guang Yong, Juhyun Lee, Wan-Teh Chang, Wei Hua, Manfred Georg, and Matthias Grundmann. 2019. MediaPipe: A Framework for Building Perception Pipelines. (2019). <https://arxiv.org/abs/1906.08172>

[27] Susana Martinez-Conde, Stephen L Macknik, and David H Hubel. 2004. The role of fixational eye movements in visual perception. *Nature reviews neuroscience* 5, 3 (2004), 229–240.

[28] Arsha Nagrani, Joon Son Chung, and Andrew Zisserman. 2017. VoxCeleb: a large-scale speaker identification dataset. *CoRR* abs/1706.08612 (2017). <http://arxiv.org/abs/1706.08612>

[29] Catherine Pelachaud and Massimo Bilvi. 2003. Modelling Gaze Behavior for Conversational Agents. 93–100. DOI: http://dx.doi.org/10.1007/978-3-540-39396-2_16

[30] Stephen M Platt, Aaron T Smith, Francisco Azuola, Norman I Badler, and Catherine Pelachaud. 1991. Structure-based animation of the human face. (1991).

[31] K R Prajwal, Rudrabha Mukhopadhyay, Vinay P. Nambodiri, and C.V. Jawahar. 2020. A Lip Sync Expert Is All You Need for Speech to Lip Generation In the Wild. In *Proceedings of the 28th ACM International Conference on Multimedia (MM '20)*. Association for Computing Machinery, New York, NY, USA, 484–492. DOI: <http://dx.doi.org/10.1145/3394171.3413532>

[32] Alexander Richard, Michael Zollhöfer, Yandong Wen, Fernando de la Torre, and Yaser Sheikh. 2021. MeshTalk: 3D Face Animation From Speech Using

- Cross-Modality Disentanglement. In *Proceedings of the IEEE/CVF International Conference on Computer Vision (ICCV)*. 1173–1182.
- [33] SL Rogers, CP Speelman, O Guidetti, and M Longmuir. 2018. Using dual eye tracking to uncover personal gaze patterns during social interaction. *Scientific Reports* 8, 1 (2018), 4271. DOI: <http://dx.doi.org/10.1038/s41598-018-22726-7> Published 2018 Mar 9.
- [34] Shuvendu Roy and Ali Etemad. 2021. Self-supervised Contrastive Learning of Multi-view Facial Expressions. In *Proceedings of the 2021 International Conference on Multimodal Interaction*. ACM, 253–257. DOI: <http://dx.doi.org/10.1145/3462244.3479955>
- [35] Kerstin Ruhland, Sean Andrist, Jeremy B. Badler, Christopher E. Peters, Norman I. Badler, Michael Gleicher, Bilge Mutlu, and Rachel McDonnell. 2014. Look me in the Eyes: A Survey of Eye and Gaze Animation for Virtual Agents and Artificial Systems. In *Eurographics*. <https://api.semanticscholar.org/CorpusID:15850172>
- [36] Neha Sahipjohn, Ashishkumar Gudmalwar, Nirmesh Shah, Pankaj Wasnik, and Rajiv Ratn Shah. 2024. DubWise: Video-Guided Speech Duration Control in Multimodal LLM-based Text-to-Speech for Dubbing. (2024). <https://arxiv.org/abs/2406.08802>
- [37] Dario Salvucci and Joseph Goldberg. 2000. Identifying fixations and saccades in eye-tracking protocols. *Proceedings of the Eye Tracking Research and Applications Symposium* (01 2000), 71–78. DOI: <http://dx.doi.org/10.1145/355017.355028>
- [38] Tayyar Sen and T. M. Megaw. 1984. The Effects of Task Variables and Prolonged Performance on Saccadic Eye Movement Parameters. *Advances in psychology* 22 (1984), 103–111. <https://api.semanticscholar.org/CorpusID:142928885>
- [39] J. Stahl. 1999. Amplitude of human head movements associated with horizontal saccades. *Experimental Brain Research* 126 (1999), 41–54. DOI: <http://dx.doi.org/10.1007/s002210050715>
- [40] Zhiyao Sun, Tian Lv, Sheng Ye, Matthieu Lin, Jenny Sheng, Yu-Hui Wen, Mingjing Yu, and Yong-Jin Liu. 2024. DiffPoseTalk: Speech-Driven Stylistic 3D Facial Animation and Head Pose Generation via Diffusion Models. *ACM Transactions on Graphics (TOG)* 43, 4, Article 46 (2024), 9 pages. DOI: <http://dx.doi.org/10.1145/3658221>
- [41] Balamurugan Thambiraja, Ikhsanul Habibie, Sadegh Aliakbarian, Darren Cosker, Christian Theobalt, and Justus Thies. 2023. Imitator: Personalized Speech-driven 3D Facial Animation. In *Proceedings of the IEEE/CVF International Conference on Computer Vision (ICCV)*. 20621–20631.
- [42] A. Vehlen, A. V. Belopolsky, and G. Domes. 2024. Gaze behavior in response to affect during natural social interactions. *Frontiers in Psychology* 15 (October 2024), 1433483. DOI: <http://dx.doi.org/10.3389/fpsyg.2024.1433483>
- [43] Suzhen Wang, Lincheng Li, Yu Ding, Changjie Fan, and Xin Yu. 2021. Audio2Head: Audio-driven One-shot Talking-head Generation with Natural Head Motion. (2021). <https://arxiv.org/abs/2107.09293>
- [44] Jinbo Xing, Menghan Xia, Yuechen Zhang, Xiaodong Cun, Jue Wang, and Tien-Tsin Wong. 2023. Codetalker: Speech-driven 3d facial animation with discrete motion prior. In *Proceedings of the IEEE/CVF Conference on Computer Vision and Pattern Recognition*. 12780–12790.
- [45] Wenxuan Zhang, Xiaodong Cun, Xuan Wang, Yong Zhang, Xi Shen, Yu Guo, Ying Shan, and Fei Wang. 2022. SadTalker: Learning Realistic 3D Motion Coefficients for Stylized Audio-Driven Single Image Talking Face Animation. *arXiv preprint arXiv:2211.12194* (2022).
- [46] Hang Zhou, Yasheng Sun, Wayne Wu, Chen Change Loy, Xiaogang Wang, and Ziwei Liu. 2021. Pose-Controllable Talking Face Generation by Implicitly Modularized Audio-Visual Representation. *CoRR* abs/2104.11116 (2021). <https://arxiv.org/abs/2104.11116>
- [47] Yang Zhou, Xintong Han, Eli Shechtman, Jose Echevarria, Evangelos Kalogerakis, and Dingzeyu Li. 2020. MakeltTalk: speaker-aware talking-head animation. *ACM Transactions on Graphics* 39, 6 (Nov. 2020), 1–15. DOI: <http://dx.doi.org/10.1145/3414685.3417774>